Observation of Turbulent-Driven Shear Flow in a Cylindrical Laboratory Plasma Device

C. Holland, J. H. Yu, A. James, D. Nishijima, M. Shimada, N. Taheri, and G. R. Tynan

Department of Mechanical and Aerospace Engineering, University of California San Diego, 9500 Gilman Drive, La Jolla, California 92093-0417, USA

(Received 20 September 2005; published 18 May 2006)

An azimuthally symmetric radially sheared plasma fluid flow is observed to spontaneously form in a cylindrical magnetized helicon plasma device with no external sources of momentum input. A turbulent momentum conservation analysis shows that this shear flow is sustained by the Reynolds stress generated by collisional drift turbulence in the device. The results provide direct experimental support for the basic theoretical picture of drift-wave–shear-flow interactions.

DOI: 10.1103/PhysRevLett.96.195002 PACS numbers: 52.35.Ra, 52.35.Kt, 52.35.Mw

It is believed that drift waves and their associated transport are the source of the unacceptably high levels of transport in tokamaks and other proposed magnetic confinement schemes for developing nuclear fusion as a practical energy source. The theoretical properties of linear drift waves are well understood and were verified in a series of experiments [1–6], and are discussed in a review paper by Horton [7]. In the last decade, extensive analytic and computational investigations of drift-wave turbulence [8–11] have suggested that the drift waves nonlinearly drive poloidally and toroidally symmetric shear flows, termed zonal flows, via the turbulent Reynolds stress; the zonal flows in turn decorrelate the turbulent spectrum and set the saturation levels of the turbulence [12]. Because of the central role drift waves play in determining overall confinement (and therefore performance) of various confinement schemes, developing a detailed first-principles understanding of the interaction between drift waves and zonal flows is therefore highly desirable. The question of nonlinearly generated zonal flows also arises in geophysical and astrophysical settings [13]; the effects of shear flows on ionospheric plasma turbulence [14] are also of interest.

Some of the strongest evidence for the existence of such flows in tokamaks has come from the application of velocity inference schemes to beam emission spectroscopy data on the DIII-D tokamak [15,16]; phase contrast imaging has also provided support for the existence of zonal flows [17]. Doppler reflectometry has been used on the ASDEX machine to provide evidence for zonal flows [18] as well. In work on the CHS device, heavy ion beam probes were used to directly measure potential fluctuations which were found to be consistent with expectations for zonal flows [19]. Probe measurements in the HT-6M tokamak device [20] show that the evolution of the turbulent Reynolds stress is consistent with the formation of the initial shear layer during a transition to improved Ohmic confinement in that device, while an examination of probe data from the CCT, PBX-M, and DIII-D devices showed that nonlinear coupling between low-frequency and higher frequency potential fluctuations exists and that this coupling evolves immediately prior to the L-H transition in the DIII-D tokamak [21,22]. In a series of papers Shats and coworkers [23–27] have shown that low-frequency oscillating shear flows exist in the H-1 heliac device, that these shear flows modulate the turbulent transport, and are sustained by a transfer of energy from higher frequency turbulent fluctuations into the low-frequency oscillations. However, the ions are unmagnetized in these experiments and thus the results may not be directly comparable to either existing theory or to expectations for large magnetic confinement experiments. The effects of sheared axial and azimuthal flows on drift waves have recently been investigated in a Q machine [28,29] where an external biasing is used to drive the flows. More generally, we note that there have been numerous studies of the effects of *externally imposed* shear flows upon turbulence (often in plasma columns similar to the ones used here; see, e.g., Refs. [6,28–30]), but comparatively few *experimental* studies of how plasma turbulence can drive shear flows, and that the previous studies have generally not investigated the transfer of energy from the fluctuations to the shear flow. In this Letter we provide evidence that a transfer of energy occurs from collisional drift turbulence fluctuations with finite frequency ($5\ \text{kHz} < f < 50\ \text{kHz}$) into linearly stable low-frequency ($f < 5\ \text{kHz}$) azimuthally symmetric radially sheared $\vec{E} \times \vec{B}$ plasma flow. Measurement of the Reynolds stress is used with the time-averaged azimuthal momentum equation to show that the observed shear flow is self-consistent with the measured turbulence profile, and is in fact nonlinearly driven by the turbulent Reynolds stress. The results provide experimental verification of shear flow generation from drift turbulence.

The results described here were carried out in the (C)ontrolled (S)hear (D)ecorrelation E(x)periment (CSDX) using Argon. The CSDX machine is a 3 m long linear plasma column within a solenoidal magnetic field of variable strength (up to 1000 G), and uses an azimuthally symmetric half-wavelength helicon antenna operating at 13.56 MHz to achieve ionization with an Argon gas pressure of 3.0 mTorr maintained during operation. It exhibits the usual signs of helicon mode operation: mean density n_0 proportional to magnetic field B, and a transition to high

density operation ($n_0 >$ few $\times 10^{12}$ cm^{-3}) for sufficiently large B fields (>400 G), source power (>1 kW), and fill pressure (>1 m Torr). The present plasma source radius is approximately 4 cm and the vacuum chamber radius is 10 cm; all data shown here were taken using a magnetic field of 1000 G and a source power of 1.5 kW, at a distance 75 cm downstream from the source. The field lines terminate on insulating surfaces in the source, and on a series of 10 concentric end rings located 160 cm downstream of the plasma source exit; in the results described here, these rings are electrically floating, prohibiting radial plasma currents (and thus azimuthally directed torques) from existing in the plasma. Detailed spatiotemporal measurements of equilibrium and fluctuating density, potential, and electron temperature are made with various moveable probe arrays, while an optical fiber array measuring plasma emissions across a central chord is used to measure line-averaged ion and neutral temperatures. The neutral argon temperature was found by measuring 750 nm Ar-I emission using a central-chord viewing optical fiber connected to a high resolution $\lambda_0/\Delta\lambda = 2.5 \times 10^5$ 10 m focal length spectrometer equipped with a 30 cm echelle grating in a Littrow configuration [31]. Higher order spectral aliasing is avoided by incorporating a bandpass interference filter at the spectrometer entrance. The measured 1.7 pm full width at half maximum Gaussian instrument response function is then deconvolved from the measured Doppler broadened Ar-I spectra to yield a line-averaged neutral temperature $T_{\text{gas}} = 0.5$ eV $\pm$ 0.15 eV; ion temperature is similarly measured via 488 nm Ar-II emission to have a value $T_i =$ 0.6 eV $\pm$ 0.15 eV. These error bars are estimated from the quality of the least squares fitting. Because the available view is a central-chord average, the azimuthal plasma rotation is not observable as a Doppler shift of the ion line. At 1000 G, the ion cyclotron frequency for Argon $\Omega_{\text{ci}} = 2.4 \times 10^5$ rad/s $(f_{\text{ci}} = \Omega_{\text{ci}}/2\pi = 38$ kHz), the sound speed $C_s = \sqrt{T_e/M_i} = 2.3 \times 10^5$ cm/s (using $T_e = 2.2$ eV), and ion-sound gyroradius $\rho_s = C_s/\Omega_{\text{ci}} =$ 1 cm; the density scale length (in the region of strongest gradient) $L_n = (d \ln n_0/dx)^{-1} \approx 2$ cm. A more detailed description of the plasma source and fluctuation characteristics can be found in the literature [32–34].

Data showing typical radial profiles of the time-averaged plasma density, particle flux, fluctuation spectra, and rms fluctuation amplitudes are shown in Fig. 1. At 1000 G, both density and $\vec{E} \times \vec{B}$ velocity ($\vec{V} = \vec{E} \times \vec{B}/B^2$) fluctuations peak at low frequencies ($f < f_{\text{ci}}$) but have a broad spectral extent as shown in Fig. 1(b); previous work has identified these fluctuations as collisional drift waves [33]. Examination of the azimuthal velocity spectrum also shows the existence of a low-frequency component ($f < 5$ kHz) which has been shown [32] to be azimuthally symmetric (i.e., mean wave number $\bar{k}_\theta = 0$); there is no correspondng signal in the density fluctuations (suggesting it is not an ion-acoustic wave). Figure 1(d) also indicates that while the finite-frequency fluctuations (those between 5 and

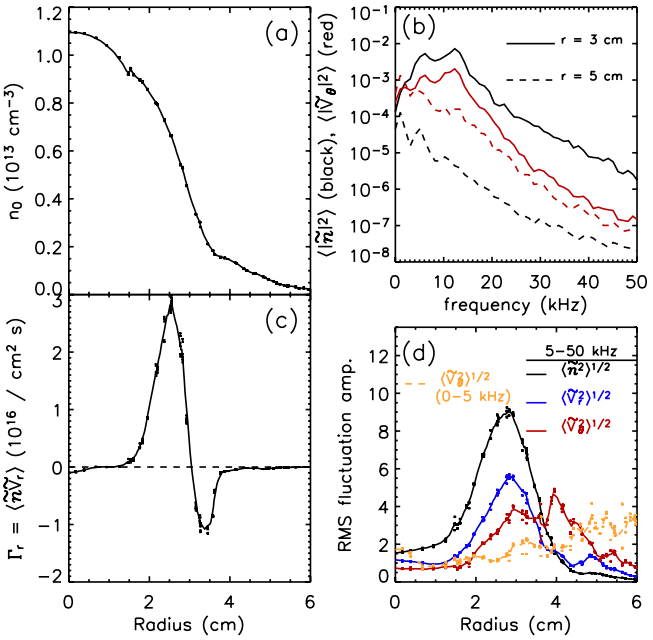

FIG. 1 (color online). (a) Time-averaged density profile, (b) frequency spectra of density (black), and azimuthal velocity (red) fluctuations, at $r = 3$ cm (solid curves) and $r = 5$ cm (dashed curves). (c) Time-averaged radial particle flux profile, and (d) rms amplitudes of density fluctuations (solid black line), radial velocity fluctuations (solid blue line), and azimuthal velocity fluctuations (solid red line) filtered between 5–50 kHz, as well as azimuthal velocity fluctuations between 0–5 kHz (dashed yellow).

50 kHz) are fairly localized near the region of maximum density gradient ($r = 3$ cm), the low-frequency V_θ fluctuation (<5 kHz) is strongest in the range of $r = 4$–6 cm. Because this low-frequency component is azimuthally symmetric and has no radial $\vec{E} \times \vec{B}$ velocity component associated with it to extract free energy from the equilibrium gradients, it is linearly stable [32] and must therefore be supported by either nonlinear mechanisms or by external torques against linear damping mechanisms. However, the insulating parallel boundary conditions rule out the possibility of external torques, suggesting that the observed low-frequency fluctuation corresponds to a nonlinearly driven, azimuthally symmetric sheared $\vec{E} \times \vec{B}$ flow.

To further quantify the underlying physics of this shear flow, we have undertaken a detailed analysis of the azimuthal momentum equation. In the presence of a finite ion-neutral momentum dissipation rate ν_{i-n} and finite ion-ion collisional viscosity μ_{ii}, the relationship between the radial profile of the azimuthal plasma fluid velocity and the turbulent Reynolds stress is given by the time-averaged azimuthal component of the ion momentum equation

$$\frac{1}{r^2}\frac{\partial}{\partial r}(r^2\langle\tilde{V}_r\tilde{V}_\theta\rangle) = -\nu_{i-n}\langle V_\theta\rangle + \mu_{ii}\left(\frac{1}{r}\frac{\partial}{\partial r}\left(r\frac{\partial\langle V_\theta\rangle}{\partial r}\right) - \frac{\langle V_\theta\rangle}{r^2}\right), \quad (1)$$

where the brackets denote a time average and tildes fluctuating quantities, such that $\langle V_\theta \rangle$ is the time-averaged azimuthal ion fluid velocity, ν_{i-n} is the ion-neutral collision rate, and μ_{ii} is the ion viscosity. In deriving Eq. (1), we have assumed that the fluctuations are incompressible, that time-averaged quantities have only a radial spatial dependence, and that ion pressure and neutral flow velocities are negligible. Using a four-tip Langmuir probe assembly (which allows us to measure density and electric field fluctuations simultaneously) we have measured the electrostatic turbulent Reynolds stress, $\langle R \rangle = \langle \tilde{E}_r \tilde{E}_\theta \rangle / B_0^2$ (equal to $-\langle \tilde{V}_r \tilde{V}_\theta \rangle$ under the assumption that the convecting velocity fluctuations are purely electrostatic) where $\tilde{E}_r = \Delta V_f / \Delta x_r$ is the fluctuating radial electric field taken as the difference between the floating potentials measured with two probe tips separated radially by a distance $\Delta x_r = 0.5$ cm; the fluctuating azimuthal electric field $\tilde{E}_\theta = \Delta V_f / \Delta x_\theta$ is measured similarly. Figure 2(a) shows the measured profile of $\langle \tilde{V}_r \tilde{V}_\theta \rangle$. All of the time-averaged data presented in this Letter was obtained by averaging approximately 32 000 points of data sampled at 1 MHz taken with the probe assembly held fixed at 193 different spatial locations. Because CSDX can operate in a steady-state fashion for much longer time scales, the statistical error bars are generally within the thickness of the plotted mean value curves.

Taking the measured Reynolds stress shown in Fig. 2(a), we can then solve the momentum equation for $\langle V_\theta \rangle$ if the viscosity and neutral damping rates are known. Using reasonable boundary conditions (i.e., $\langle V_\theta \rangle \to 0$ at $r = 0$) the solution can be found numerically by using the measured profiles and radially integrating Eq. (1). For the measured ion and neutral gas temperatures we estimate an average ion viscosity $\mu_{ii} = 0.3 \rho_i^2 \nu_{ii} \approx 4 \times 10^4$ cm^2/ sec . The gas pressure is measured to be 3 mTorr at the device wall, via a capacitance manometer. Assuming the gas pressure is uniform through the plasma column, and taking the on-axis gas temperature to be given by the measured chord-averaged value $T_{\text{gas}} = 0.5$ eV given earlier, we estimate the on-axis neutral density to be $n_{\text{gas}} = 4 \times 10^{12}$ cm^{-3}. A more detailed discussion of this estimate is given elsewhere [34]. Using published data for the total ion-neutral scattering cross section for argon [35] (i.e., including both charge exchange and elastic collisions) we then estimate that the ion-neutral momentum damping rate $\nu_{i-n} \equiv n_{\text{gas}} V_{\text{th}_i i} (\sigma_{io}^{\text{CX}} + \sigma_{io}^{\text{elas}}) \approx 6 \times 10^3$ sec^{-1}. Because the ion and neutral temperatures are likely to be peaked at $r = 0$ and because the plasma density and neutral density have significant spatial profiles, these values for μ_{ii} and ν_{i-n} likely have significant spatial variations. For a uniform ion-neutral flow damping rate $\nu_{i-n} = 6 \times 10^3$ sec^{-1} and a viscosity profile given as $\mu_{ii} = 4 \times 10^4$ cm^2/ sec for the region $r < 3.25$ cm and $\mu_{ii} = 4 \times 10^3$ cm^2/ sec for $r > 3.25$ cm [shown in Fig. 2(b), consistent with the mean density and ion temperature decreasing with r, since $\mu_{ii} \propto n T_i^{-1/2}$], this turbulent momentum balance analysis gives the time-averaged azimuthal ion fluid velocity profile shown as the solid curve in Fig. 3.

Because Eq. (1) describes a linear (albeit complex) relationship between the Reynolds stress and $\langle V_\theta \rangle$, and the statistical error in our Reynolds stress profile measurement is negligible, we expect that the corresponding statistical error in our predicted $\langle V_\theta \rangle$ profile is correspondingly small. However, there are several possible systematic errors which may provide more serious error in the predicted $\langle V_\theta \rangle$ profile. First is the uncertainty in the dissipation profiles, which arises from the fact that spatial profiles of ion temperature, neutral density, and neutral temperature are unavailable. In general, it was found that the magnitude of $\langle V_\theta \rangle$ was inversely proportional to the magnitude of μ_{ii}, and had a somewhat complex dependence on the spatial profile of μ_{ii}; $\langle V_\theta \rangle$ was much less sensitive to the magnitude and profile of ν_{i-n} and so we therefore used a spatially uniform profile for ν_{i-n} in the interest of simplicity, as no measurements of the neutral profiles are available. The

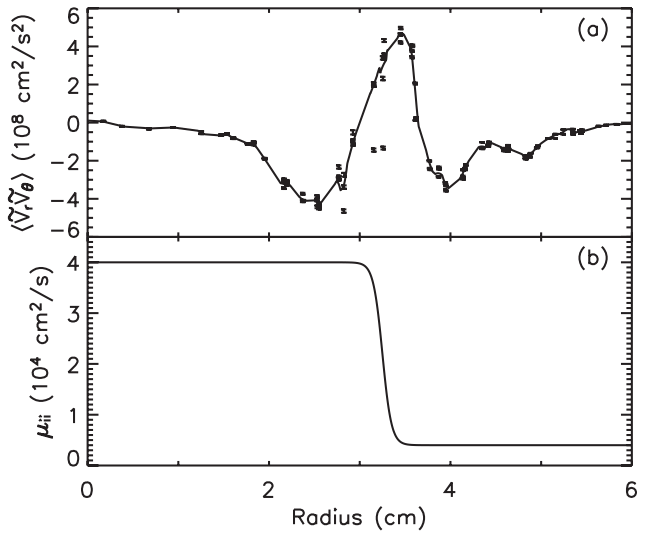

FIG. 2. (a) Radial profile of turbulent Reynolds stress $\langle \tilde{V}_r \tilde{V}_\theta \rangle$. (b) Radial profile of ion viscosity used in momentum balance.

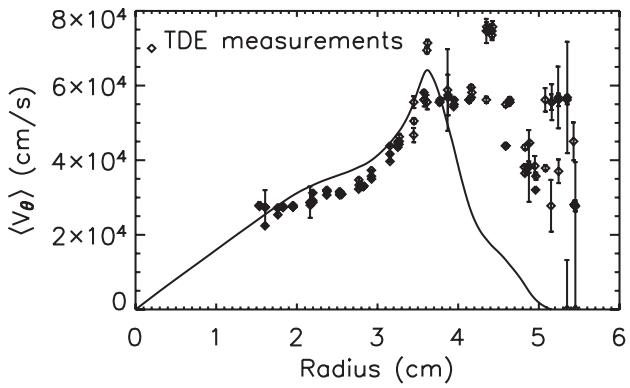

FIG. 3. Mean azimuthal velocity profile predicted by force balance (solid line), and measured via time-delay estimation (diamonds).

second potential source of systematic error is our neglect of electron temperature fluctuations in converting the floating potential measured by the Langmuir probes to plasma potential [36]. We are unaware of any scheme that allows for simultaneous measurement of temperature and plasma potential fluctuations, which would allow us to correct for this effect.

We have also measured the radial profile of the mean azimuthal plasma velocity using time-delay estimation techniques [15,16]. In this technique the density (or potential) fluctuations at two azimuthal positions separated by 0.5 cm are sampled with high time resolution (1 MHz) and then the small time delay incurred by the propagation of the fluctuations between the two probes is measured by determining where the cross-correlation function peaks. The velocity is then taken as the spatial separation divided by this measured time delay. The results are shown as the diamonds in Fig. 3, and are in very good agreement with the flow that is maintained by the turbulent Reynolds stress. The azimuthal velocity has a strong radial variation and is peaked at $r \approx 3.6$ cm, indicating the presence of a plasma shear layer at this location, consistent with the previous measurements shown in Figs. 1(c) and 1(d) and consistent with the location of the particle flux transport barrier. When combined with previous observations, these results show that a velocity shear layer exists in this plasma (which has no external sources of momentum such as a cathode-anode cross-field current), that the velocity shear layer is azimuthally symmetric and therefore linearly stable, and is consistent with the measured Reynolds stress and damping mechanisms. Taken together, these observations indicate that a turbulent-driven zonal flow coexists with the drift turbulence in this device, and so provide essential experimental support for the theoretical features of zonal flow generation from drift-wave turbulence in magnetized plasmas [12].

The authors wish to thank P. H. Diamond, S.-I. Itoh, K. Itoh, and J. Boedo for many valuable suggestions and conversations. Discussions with S.-I. Itoh and K. Itoh were made possible by the Grant-in-Aid for Specially-Promoted Research of MEXT Japan (16002005). This research was performed under Grants No. DE-FG02-04ER54773 and No. DE-FG02-04ER54734. C. Holland performed this research under an appointment to the Fusion Energy Postdoctoral Research Program, administered by the Oak Ridge Institute for Science and Education under Contract No. DE-AC05-00OR22750 between the U.S. Department of Energy and Oak Ridge Associated Universities.

[1] H. W. Hendel, T. K. Chu, and T. C. Simonen, Phys. Fluids **11**, 2426 (1968).
[2] T. K. Chu, B. Coppi, H. W. Hendel, and F. W. Perkins, Phys. Fluids **12**, 203 (1969).
[3] P. Politzer, Phys. Fluids **14**, 2410 (1971).
[4] F. F. Chen, Phys. Fluids **7**, 949 (1964).
[5] F. F. Chen, Phys. Fluids **8**, 752 (1965); F. F. Chen, Phys. Fluids **8**, 912 (1965); F. F. Chen, Phys. Fluids **8**, 1323 (1965).
[6] F. F. Chen, Phys. Fluids **9**, 965 (1966).
[7] W. Horton, Rev. Mod. Phys. **71**, 735 (1999).
[8] P. H. Diamond *et al.*, *Proceedings of the 17th IAEA Fusion Energy Conference, Yokohama, Japan, 1998* (IAEA, Vienna, 1998), CD-ROM file TH3/1, http://www.iaea.org/programmes/ripc/physics/start.htm.
[9] G. W. Hammett *et al.*, Plasma Phys. Controlled Fusion **35**, 973 (1993).
[10] Z. Lin *et al.*, Science **281**, 1835 (1998).
[11] J. Candy and R. E. Waltz, J. Comput. Phys. **186**, 545 (2003).
[12] P. H. Diamond, S. I. Itoh, K. Itoh, and T. S. Hahm, Plasma Phys. Controlled Fusion **47**, R35 (2005).
[13] F. H. Busse, Chaos **4**, 123 (1994).
[14] P. M. Kintner and C. E. Seyler, Space Sci. Rev. **41**, 91 (1985).
[15] M. Jakubowski, R. J. Fonck, and G. R. McKee, Phys. Rev. Lett. **89**, 265003 (2002).
[16] G. R. McKee *et al.*, Phys. Plasmas **10**, 1712 (2003).
[17] S. Coda, M. Porkolab, and K. H. Burrell, Phys. Rev. Lett. **86**, 4835 (2001).
[18] G. D. Conway *et al.*, Plasma Phys. Controlled Fusion **47**, 1165 (2005).
[19] A. Fujisawa *et al.*, Phys. Rev. Lett. **93**, 165002 (2004).
[20] Y. H. Xu *et al.*, Phys. Rev. Lett. **84**, 3867 (2000).
[21] G. R. Tynan, R. A. Moyer, M. J. Burin, and C. Holland, Phys. Plasmas **8**, 2691 (2001).
[22] R. A. Moyer, G. R. Tynan, C. Holland, and M. J. Burin, Phys. Rev. Lett. **87**, 135001 (2001).
[23] M. G. Shats and W. M. Solomon, Phys. Rev. Lett. **88**, 045001 (2002).
[24] M. G. Shats and W. M. Solomon, New J. Phys. **4**, 30 (2002).
[25] H. Xia and M. G. Shats, Phys. Rev. Lett. **91**, 155001 (2003).
[26] H. Xia and M. G. Shats, Phys. Plasmas **11**, 561 (2004).
[27] M. G. Shats, H. Xia, and H. Punzmann, Phys. Rev. E **71**, 046409 (2005).
[28] M. E. Koepke *et al.*, Phys. Plasmas **9**, 3225 (2002).
[29] E. W. Reynolds, T. Kaneko, M. E. Kopke, and R. Hatakeyama, Phys. Plasmas **12**, 072103 (2005); T. Kaneko, E. W. Reynolds, R. Hatakeyama, and M. E. Kopeke, Phys. Plasmas **12**, 102106 (2005).
[30] D. L. Jassby, Phys. Fluids **15**, 1590 (1972).
[31] G. R. Harrison, J. Opt. Soc. Am. **39**, 522 (1949); G. R. Harrison, J. E. Archer, and J. Camus, J. Opt. Soc. Am. **42**, 706 (1952).
[32] G. R. Tynan *et al.*, Phys. Plasmas **11**, 5195 (2004).
[33] M. Burin, G. Antar, N. Crocker, and G. R. Tynan, Phys. Plasmas **12**, 052320 (2005).
[34] G. R. Tynan *et al.*, Plasma Phys. Controlled Fusion **48**, S51 (2006).
[35] E. W. McDaniel, J. B. A. Mitchell, and M. E. Rudd, *Atomic Collisions: Heavy Particle Projectiles* (Wiley, New York, 1983).
[36] R. A. Moyer *et al.*, Phys. Plasmas **2**, 2397 (1995).